DOI: 10.1002/ejic.200900609

Dinuclear Manganese and Cobalt Complexes with Cyclic Polyoxovanadate Ligands: Synthesis and Characterization of $[Mn_2V_{10}O_{30}]^{6-}$ and $[Co_2(H_2O)_2V_{10}O_{30}]^{6-}$

Shinnosuke Inami,[a] Masaki Nishio,[a] Yoshihito Hayashi,*[a] Kiyoshi Isobe,[a] Hiroyuki Kameda,[b] and Tatsuya Shimoda[b,c]

Keywords: Polyoxometalates / Oxido ligands / Vanadates / Cobalt / Manganese

An all-inorganic complex, $[Mn_2\{(VO_3)_5\}_2]^{6-}$ (**1**), was synthesized, and the structure determination reveals a dinuclear manganese complex coordinated by two cyclic pentavanadate ligands. The cyclic pentavanadate units sandwich the edge-sharing octahedral dimanganese core through coordination of the oxido group of the pentavanadate. A dinuclear cobalt complex with a cyclic decavanadate, $[Co_2(OH_2)_2(VO_3)_{10}]^{6-}$ (**2**), was also synthesized. The structure analysis reveals a dinuclear cobalt complex with a macrocyclic decavanadate, which is composed of 10 VO_4 units joined by the vertex sharings. The CoO_6 octahedrons are edge-shared, with each cobalt octahedron coordinated to five oxido groups from the decavanadate. The remaining site is occupied by water. The coordinated water molecules are supported with hydrogen bonds in two directions. Complex **2** in acetonitrile shows no reactivity with dioxygen even at low temperature, and the cyclic voltammogram of **2** shows no redox chemistry in acetonitrile. Complex **2** exhibits chromism by water exposure both in the solid state and in acetonitrile. Complex **2** is green–yellow in color, and the addition of water causes the complex to turn brown. After heating the sample, it returns to its original color in a reversible manner. The EXAFS data in acetonitrile is also reported and is consistent with the solid-state structure.

Introduction

Polyoxometalates exhibit a variety of coordination abilities as building blocks of molecular-based materials with a diverse range of structural versatility.[1] The negatively charged polyoxometalate can serve as an inorganic ligand that is able to form a metal complex through the coordination of the oxido groups. The typical heteropolyoxometalates, such as Anderson-type compounds, may be regarded as all-inorganic metal complexes (Figure 1). Other examples of all-inorganic complexes have been reported for $[Mn(Nb_6O_{19})_2]^{12-}$ and its Ni^{IV} isomorph.[2] Since the discovery of cation–anion complex formation in polyoxometalate chemistry, a variety of complex formations have been investigated.[3] The introduction of heteroatoms in the polyoxometalate frameworks can introduce chirality into the structure, and recently the chirality of sandwich and substituted lacunary type polyoxometalate derivatives has been reviewed.[4] The lacunary polyanions are good ligands at their vacant sites, and they have been utilized as all-inorganic ligands for lanthanide ions.[5] Recently, we studied the coordination chemistry of polyoxometavanadate species that have the capability to coordinate to Cu^{2+}, Ni^{2+}, and Pd^{2+} cations.[6] Large cyclic polyoxovanadates act as macrocyclic ligands for transition-metal cations. In the all-inorganic complex, the ligands are constructed by a $[(VO_3)_n]^{n-}$ anion that is composed of a ring of vertex-shared VO_4 units forming a crown-ether-type cyclic structure. The coordination of the oxido groups to the heterometal ion produces the all-inorganic polyoxovanadate complex. The chemistry between cyclic metavanadates and heterometal cations defines a new class of heteropolyoxometalates.[7] We describe here two types of structurally novel dinuclear complexes of manganese and cobalt with cyclic $[(VO_3)_n]^{n-}$ ligands. Both complexes have an edge-shared dinuclear octahedral unit, and the coordination mode of the polyoxovanadates shows a striking contrast between the dimanganese and dicobalt complexes. The dimanganese unit has a sandwich structure between the two cyclic pentavanadates through the coordination of the oxido groups of the pentavanadates. In contrast, the dicobalt unit is surrounded by the cyclic decavanadate, which resembles a crown-ether-type macrocyclic complex. Both compounds are thermally stable and soluble in acetonitrile. The cobalt complex shows chromism with exposure to water and removal of water returns the complex

[a] Department of Chemistry, Graduate School of Natural Science and Technology, Kanazawa University,
Kakuma, Kanazawa 920-1192, Japan
Fax: +81-76-264-5742
E-mail: hayashi@kenroku.kanazawa-u.ac.jp
[b] JST, ERATO, Shimoda Nanoliquid Process Project,
2-5-3 Asahidai, Nomi-shi, Ishikawa 923-1211, Japan
[c] School of Material Science, Japan Advanced Institute of Science and Technology (JAIST),
1-1 Asahidai, Nomi, Ishikawa 923-1292, Japan

to its original color. Extended X-ray absorption fine structure (EXAFS) studies are also performed in acetonitrile solution.

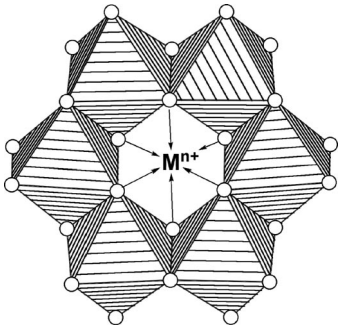

Figure 1. Alternative view of Anderson-type polyoxometalate. MO_6 units are represented by hatched octahedrons. Oxygen atoms are represented by plain circles.

Results and Discussion

Synthesis

Reactions of metavanadate with Mn^{2+}, Fe^{2+}, and Co^{2+} were surveyed in this paper. Treatment of $[Mn(CH_3CN)_4]^{2+}$ and $[VO_3]^-$ ions[8] in acetonitrile formed $[Mn_2\{(VO_3)_5\}_2]^{6-}$ (**1**) in 75% yield. If aqueous manganese ions were used in the synthesis, insoluble materials precipitated and **1** was not formed. The formation of the sandwich-type complex contrasts with the case of Cu^{2+}, Ni^{2+}, and Pd^{2+} cations, where all the obtained complexes were crown-ether-type macrocyclic complexes.[6] In Cu^{2+} and Pd^{2+} complexes, the heteropolyoxovanadate complexes incorporated the metal cations without the coordination of hydroxide or water ligands. In the Ni^{2+} complex, the hydrolysis reaction caused the formation of a hydroxido-bridged nickel(II) tetramer, and the resulting heteropolyoxometalate incorporated the hydroxido-bridged tetramer with the coordination of water ligands. In complex **1**, instead of incorporating a heteroatom at the center of the ring, the small cyclic pentavanadate acted as a sandwich ligand to the dimanganese core. The reaction between $[Co(CH_3CN)_6]^{2+}$ and $[VO_3]^-$ in acetonitrile produced the novel complex $[Co_2(H_2O)_2(VO_3)_{10}]^{6-}$ (**2**), which has a macrocyclic decavanadate ligand. When a Co^{II} aqua complex was employed, the reaction produced the cobalt complex $[CoCl(V_4O_{12})]^{3-}$, where the CoCl group was attached on the surface of the cyclic tetravanadate anion.[9] The tetravanadate ring was too small to be a macrocyclic ligand. Nonaqueous conditions are required for the synthesis of these complexes. In both complexes, the electrostatic charges that were built up on the cyclic vanadate rings were compensated by the dinuclear transition-metal cations. The synthesis of an iron(II) complex was not successful. The addition of $[Fe(CH_3CN)_6]^{2+}$ to the acetonitrile solution of $[VO_3]^-$ immediately produced a purple-colored solution. Iron(II) acted as a reducing reagent to the vanadate species, which resulted in the isolation of the reduced decavanadate ion $[V_{10}O_{26}]^{4-}$.[10]

IR Spectroscopy

The IR spectra of **1** and **2** showed similar characteristic features of the macrocyclic polyoxovanadate complexes with multiple appearances of V–O stretches in the region 500–1000 cm^{-1}. The strong bands in the range 900–970 cm^{-1} correspond to the $\nu(V{=}O_{terminal})$ stretching frequencies (Figure 2). A notable feature is the splittings of those peaks over a wide range.

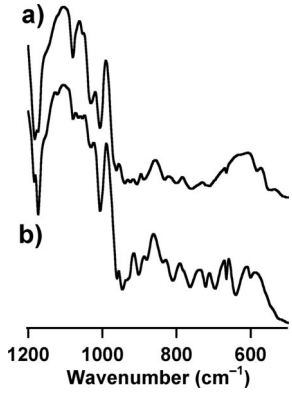

Figure 2. Infrared spectra of (a) complex **1** and (b) complex **2**.

The typical isopolyoxovanadates only show a single $\nu(V{=}O_{terminal})$ peak, reflecting the uniform VO_x polyhedron. The distortion of the VO_4 units by coordination to the different sites of the heterometals is responsible for these splittings. The coordination of the cyclic vanadate ligands causes the formation of two types of μ^2-O bridges, for example, V–O–V and V–O–M, where M is a heteroatom. The multiple stretchings spanning the range 600–900 cm^{-1} are consistent with the structures of complexes **1** and **2**, which contain the two types of μ^2-O bridges.

Structures

Figure 3 shows the structure of anion **1** in ORTEP and polyhedral views. An inversion center relates the sandwiched molecule. The MnO_6 octahedrons of the dinuclear manganese cores are edge-shared and bridged by O2. The remaining manganese coordination sites are occupied by the oxido groups from the cyclic pentavanadate. Each VO_4 unit has one terminal oxygen atom, two bridging oxygen atoms between the vanadium atoms, and one bridging oxygen atom to the manganese atom. The pentavanadate rings are composed of vertex-shared tetrahedrons of VO_4 units and they act as a pentadentate ligand that coordinates to the dimanganese unit through the O1, O2, O3, O6, and O7 atoms. The Mn–O distances of the μ^3-O bridging oxygen atom are longer [2.211(2) and 2.213(2) Å] than the Mn–O distances of the μ^2-O oxygen atom (average distance is 2.151 Å). The separation of manganese atoms is 3.308(2) Å. The vanadium atoms of V1, V3, V4, and V5 lie on the same plane, and the V2 unit is inclined toward the manganese octahedron; the distance to the least square plane is 0.737 Å. The distance between the plane and Mn1 is 2.993 Å. The packing water molecule has a close contact

with O14 [O14···O16 2.895(3) Å]. Two acetonitrile molecules are located in the asymmetric unit, and the methyl group points in the direction of anion **1**. The short intermolecular interactions of the methyl carbon atom and the terminal oxygen atoms are observed in the length of 3.016(5) Å (O15···C20) at the manganese bridging VO_4 group. The others have lengths of 3.260(4) Å (O14···C20).

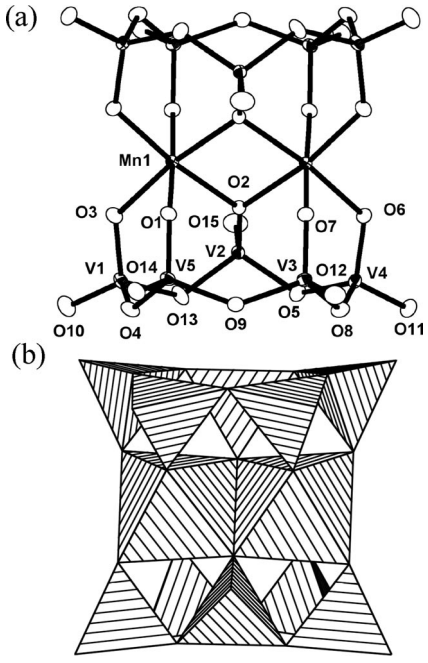

Figure 3. (a) Thermal ellipsoidal plot of anion **1** with the atom numbering scheme; (b) polyhedral representation of anion **1**. Octahedrons are MnO_6 units and tetrahedrons are VO_4 units.

In complex **2**, the edge-shared octahedrons of the Co^{II} centers are coordinated by the eight oxido groups from the cyclic decavanadate, as shown in Figure 4. An inversion center relates dinuclear complex **2** with the macrocyclic decavanadate. Two of the tetrahedrons out of the ten VO_4 units are not involved in the coordination to cobalt atoms (V2 units). The O9 oxygen atom is assigned to a H_2O ligand, which is deduced from bond valence sum calculations,[11] and the positions of these protons are successfully located from the difference Fourier map and refined. The water ligands have close contacts along two directions indicating hydrogen bonds. One is to the terminal oxido (O16) of the V1 unit where the O9···O16 distance is 2.812(2) Å. The other is to the *cis*-axial oxygen (O3) of the edge-shared dinuclear cobalt units, and the distance between the water oxygen and the *cis*-axial oxygen at the octahedron is 2.711(3) Å. These hydrogen bonds in two directions seem to bind the water molecules effectively. In fact, complex **2** could be formed in the reaction system containing a trace amount of water in distilled acetonitrile. Although the highest oxidation polyoxometalate core provides a robust structural framework for the potential use of cobalt(II) complex **2** for a dioxygen activation site,[12] **2** shows no reactivity to dioxygen. This is due to the high negative charges on the anion, unlike the traditional cationic dinuclear cobalt complexes, which have been known to show various types of reactivities to dioxygen.[13] The complex shows no redox waves by means of cyclic voltammetry in the range ±2 V vs. Ag/Ag^+.

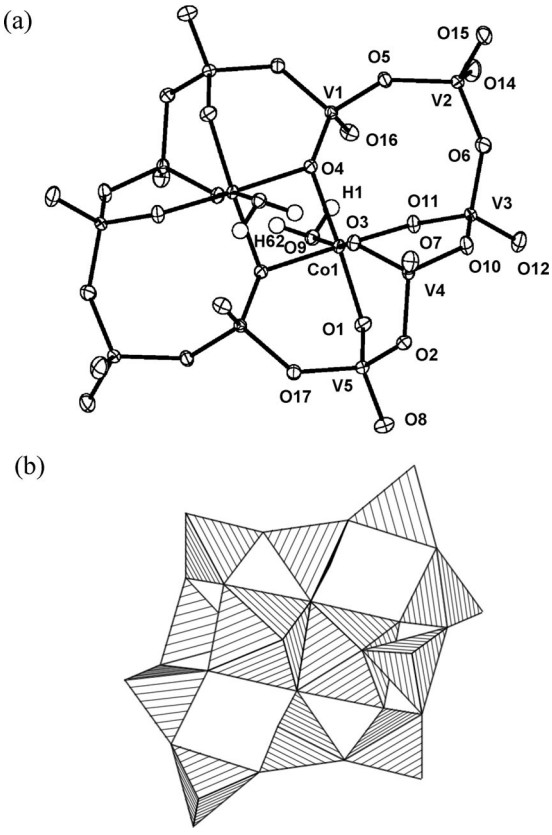

Figure 4. (a) Thermal ellipsoidal plot of anion **2** with the atom numbering scheme; (b) polyhedral representation of anion **2**. Octahedrons are $CoO_5(OH_2)$ units and tetrahedrons are VO_4 units.

Complex **2** has a green–yellow color in the solid state under dry air and its reflectance spectrum at room temperature shows a broad absorption band in the region 550–800 nm, as shown in Figure 5. The exposure of water vapor to the solid of **2** resulted in a change in color to brown. The intensity of the absorption at λ_{max} = 731 nm was greatly diminished. After heating the water-exposed sample, the original green–yellow color was restored. Complex **2** is substantially stable thermally as well as to exposure to water. The color change may be interpreted by the partially dissociated crown-like decavanadate ligands, which provide additional coordination sites to the water.

The UV/Vis spectrum recorded in acetonitrile solution displays the typical spectrum of an octahedral Co^{II} complex with a band at 744 nm (ε = 170 $mol^{-1}\,dm^3\,cm^{-1}$). The addition of water also caused a decrease in the band at 744 nm, and the color of the solution changed from green–yellow to brown. Complete removal of the solvents and heating of the powder at 100 °C returns the color to green–yellow. The powder sample of **2** shows two weight loss steps in the TG curve. The first weight loss of 2% in the tempera-

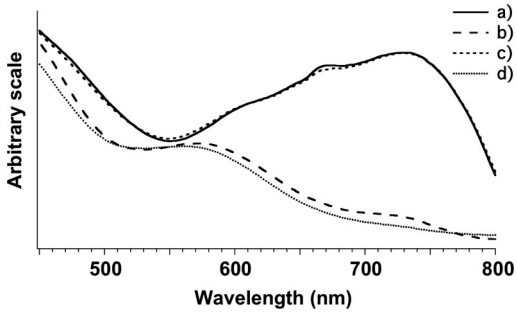

Figure 5. Electronic reflectance spectral changes of **2**, demonstrating the quasireversible chromism of the solid by exposure to water vapor. The band at λ_{max} = 731 nm decreases upon exposure to water vapor. (a) Complex **2**; (b) after exposure of the solid to water vapor; (c) after heating the water exposed sample of (b); (d) after second exposure of water vapor to (c).

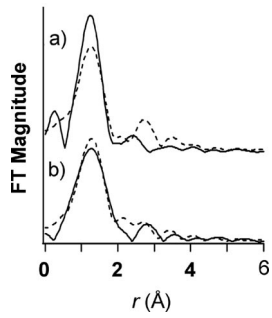

Figure 6. V-K-edge Fourier transform of **1** (a) and **2** (b) in acetonitrile. Experimental data are shown as solid lines and simulated data are in dotted lines.

ture range 40–130 °C is attributed to the loss of two coordinated water molecules (calcd. 1.9%). The loss of these two water molecules causes an increase in brightness of the green–yellow color, but the process was highly sensitive to water even in air and we were unable to record a spectrum of dried sample. The second weight loss of 40% in the temperature range 210–370 °C may be due to decomposition of the Et_4N^+ countercations.

Figure 6 shows the Fourier transforms of the EXAFS data of **1** and **2** in acetonitrile solution. The fitting parameters of the EXAFS results are presented in Table 1. The coordination numbers are fixed to the number of neighbors for each combination of the coordination spheres from single-crystal X-ray studies. The V-K-edge analyses of the complexes are consistent with the VO_4 tetrahedral geometry of the first coordination spheres. The V–O bond lengths of the fitted data correspond to the average of the V–O distances from the terminal and bridging oxygen atoms, and the lengths between complexes **1** and **2** coincide. The structure of the cyclic inorganic framework may be less rigid than that of the spherical structures.[14] The structural fluctuation may be the cause of the weak intensities of the peaks in the range 2–4 Å, and the larger Debye–Waller factor. The fitted data exhibits similar V···V lengths in **1** and **2** and indicates that both complexes are composed of cyclic structures based on the linkages of the VO_4 tetrahedra. The solubility requirements and the quality of the data limit us from drawing a definite conclusion of the structures of these complexes in solution, but the fits of the EXAFS results were consistent with the structure in the solid state. The longer V···Co distances compared to the V···Mn distances are in good agreement with the structural requirements that **1** has shorter V···Mn lengths and **2** has a noncoordinated VO_4 (V2) group that causes the longer average distances between Co and V. To monitor the chromism of complex **2**, we attempted to collect data on a water-diluted sample of **2** in acetonitrile. Unfortunately, the solubility of the diluted sample prevented us from collecting high-resolution data. Further studies should reveal the hydrated structures of **2** by means of elongation of the average V···Co distances by varying the amount of water in the solution.

Table 1. EXAFS best-fit parameters for **1** and **2** in acetonitrile. ΔE is the edge position relative to the photoelectron wavevector (eV); r is the distance in Å, and DW is the Debye–Waller Factor terms in Å^2.

	CN	r (Å)	ΔE (eV)	DW (Å^2)
Complex **1**				
V–O	4	1.70	–0.3	0.11
V–V	2	3.18	–7.0	0.11
V–O	2	3.32	–6.4	0.09
V–Mn	1	3.38	32	0.15
Complex **2**				
V–O	4	1.70	–4.2	0.11
V–V	2	3.20	3.2	0.2
V–Co	1	3.43	–3.8	0.2
V–O	1	3.47	–5.2	0

Conclusions

In conclusion, two types of all-inorganic complexes of cyclic polyoxovanadate, bispentavanadate dimanganese complex (**1**) and cyclic decavanadate dicobalt complex (**2**), were synthesized and characterized. The structure analyses reveal that complex **1** has a dinuclear framework sandwiched by cyclic petavanadates, and complex **2** was also a dinuclear cobalt complex of cyclic decavanadate ligand, which resembles a crown ether. Both of the all-inorganic ligands are constructed from cyclic polyoxovanadates through linkages of the tetrahedral VO_4 units. This new approach to all-inorganic synthesis has considerable promise for the assembly of various types of robust transition-metal complexes without organic ligands. The synthetic and chemical flexibilitiy of heteropolyoxometalates allow the tunings of metal compositions and structures exactly. The all-inorganic complex may be regarded as an ultimate basic precursor of metal oxides for electronic devices.[15]

Experimental Section

General Methods: IR spectra were recorded by mineral oil with a Horiba FT720 FTIR spectrophotometer. UV/Vis spectra and diffuse reflectance spectrum were recorded with a Hitachi U3500 spectrophotometer. Electrochemical data were recorded in acetonitrile, with 0.1 M tetra-*n*-butylammonium tetrafluoroborate salt as the supporting electrolyte. Cyclic voltammetry was carried out with

Table 2. Crystal data for **1** and **2**.

	1	**2**
Formula	$(Et_4N)_6[Mn_2(V_5O_{15})_2]\cdot 2CH_3CN\cdot 2H_2O$	$(Et_4N)_6[Co_2(H_2O)_2V_{10}O_{30}]$
Crystal system	monoclinic	monoclinic
Space group	$P2_1/c$	$P2_1/n$
a (Å)	14.044(2)	13.981(2)
b (Å)	24.465(3)	19.701(2)
c (Å)	13.820(2)	14.261(2)
α (°)	90	90
β (°)	118.968(2)	96.663(2)
γ (°)	90	90
V (Å^3)	5669(1)	3901.5(8)
Z	2	4
No. of data collected	41158	39752
No. of data used	9053	8508
No. of variables	470	451
$R(R_w)$	0.0355(0.0386)	0.0351(0.0925)
GOF	1.028	1.04

an ALS Model 600A instrument by using a standard three-electrode cell with a glassy carbon electrode, a Pt counter electrode, and a Ag/Ag^+ reference electrode. TG measurements were conducted in a Seiko TA station SSC 5000 system. Elemental analyses were performed by the Research Institute for Instrumental Analysis at Kanazawa University.

Synthesis: All reagents were reagent grade and used without further purification. Solvents were dried and distilled, then stored under an atmosphere of nitrogen. $(Et_4N)[VO_3]$, $[Mn(CH_3CN)_4](BF_4)_2$, and $[Co(CH_3CN)_6](BF_4)_2$ were synthesized by a literature procedure.[16] All synthetic procedure were performed in a glove box under an atmosphere of nitrogen gas.

$(Et_4N)_6[Mn_2\{(VO_3)_5\}_2]$ (1): To a stirred solution of $(Et_4N)[VO_3]$ (206 mg, 0.9 mmol) in acetonitrile (3 mL) was added $[Mn(CH_3CN)_4](BF_4)_2$ (39 mg, 0.1 mmol) in acetonitrile (3 mL). Slow addition of the solution was required to prevent the formation of undissolved materials. The red solution was filtered and concentrated to 2 mL. The red crystals were collected after 2 d. Yield: 70 mg (74.8% based on Mn). IR (nujol): $\tilde{\nu}$ = 962 (m), 939 (s), 923 (s), 906 (s), 889 (s), 831 (s), 800 (s), 759 (s), 711 (s), 665 (m), 582 (m), 549 (s) cm^{-1}. $(Et_4N)_6[Mn_2\{(VO_3)_5\}_2]\cdot 2CH_3CN\cdot 2H_2O$ (1998.9) calcd. C 31.25, H 6.55, N 5.60; found C 31.00, H 6.39, N 5.40.

$(Et_4N)_6[Co_2(H_2O)_2(VO_3)_{10}]$ (2): To a stirred solution of $(Et_4N)[VO_3]$ (130 mg, 0.56 mmol) in acetonitrile (2 mL) was added a solution of $[Co(CH_3CN)_6](BF_4)_2$ (46 mg, 0.96 mmol) in acetonitrile (2 mL). The green solution was filtered and concentrated to 2 mL. The green crystals were collected after 2 d. Yield: 70 mg (75.6% based on Co). IR (nujol): $\tilde{\nu}$ = 960 (m), 944 (s), 933 (sh.), 902 (m), 881 (w), 836 (w), 809 (m), 763 (s), 721 (s), 696 (s), 665 (m), 640 (s), 599 (w) cm^{-1}. $(Et_4N)_6[Co_2(H_2O)_2(VO_3)_{10}]$ (1924.8) calcd. C 29.95, H 6.49, N 4.37; found C 29.89, H 6.44, N 4.53.

EXAFS Studies: The extended X-ray analysis fine structure (EXAFS) data were collected with the synchrotron beamline BL01B1 at SPring-8 (Himeji, Japan). The spectra for V-K edges (5.464 keV) were recorded in transmission mode at room temperature by using a double-crystal Si(111) monochromator. X-rays were detected by two ion chambers, which were purged with a mixture of 70% He and 30% N_2 in ion chamber I0 and 100% N_2 in ion chamber I1, respectively. The samples in acetonitrile were sealed in a transparent plastic bag with approximate thickness of 3 mm through a handmade cell. The data analysis and handling were performed with the program package REX2000 (Rigaku). The EXAFS spectra were analyzed by using the FEFF8 code of the University of Washington analysis programs for ab initio calculation of scattering paths.[17]

X-ray Crystallography: The intensity data were collected at –150 °C with a Rigaku/MSC Mercury diffractometer with graphite monochromated Mo-K_α radiation (λ = 0.71070 Å) by using 0.5° ω-scans at 0° and 90° in ϕ. The crystal data are summarized in Table 2. Data were collected and processed by using the CrystalClear program (Rigaku).[18] The data were corrected for Lorenz and polarization effects Absorption Corrections were applied based on the face-indexing. The structures were solved by direct methods (SHELXS-86). The non-hydrogen atoms were refined anisotropically. Hydrogen atoms of water in **2** were located in the difference map, and were refined. The hydrogen atoms of the countercations and solvent molecules were positioned with idealized geometry and refined by using a riding model. The SHELX-97 program[19] was used for full-matrix least-squares refinements against F^2. CCDC-737790 (for **1**) and -737791 (for **2**) contain the supplementary crystallographic data for this paper. These data can be obtained free of charge from The Cambridge Crystallographic Data Centre via www.ccdc.cam.ac.uk/data_request/cif.

Acknowledgments

The author thanks Dr. Tomoya Uruga [Japan Synchrotron Radiation Research Institute (JASRI)] for his support in the XANES and EXAFS studies, as well as for useful discussions.

[1] M. T. Pope in *Heteropoly and Isopoly Oxometalates*, Springer, Berlin, **1983**, ch. 5.
[2] a) B. W. Dale, M. T. Pope, *Chem. Commun. (London)* **1967**, 792–793; b) C. M. Flynn Jr., G. D. Stuky, *Inorg. Chem.* **1969**, *8*, 332–334.
[3] a) Polyoxometalate special issue: C. Hill (Guest Ed.), *Chem. Rev.* **1998**, issue 1; b) J. J. Borras-Almenar, E. Coronado, A. Müller, M. T. Pope (Eds.), *Polyoxometalate Molecular Science*, NATO Science Series, Kluwer Academic Publishers, Dordrecht, **2003**, vol. 98.
[4] B. Hasenknopf, K. Micoine, E. Lacôte, S. Thorimbert, M. Malacria, R. Thouvenot, *Eur. J. Inorg. Chem.* **2008**, 5001–5013.
[5] a) B. S. Bassil, M. H. Dickman, B. Von Kammer, U. Kortz, *Inorg. Chem.* **2007**, *46*, 2452–2458; b) C. Zhang, R. C. Howell, Q.-H. Luo, H. L. Fieselmann, L. J. Todaro, L. C. Francesconi, *Inorg. Chem.* **2005**, *44*, 3569–3578; c) Q. Luo, R. C. Howell, J. Bartis, M. Dankova, W. D. Horrocks Jr., A. L. Rheingold, L. C. Francesconi, *Inorg. Chem.* **2002**, *41*, 6112–6117; d) Q.

Luo, R. C. Howell, M. Dankova, J. Bartis, C. W. Williams, W. D. Horrocks, V. G. Young, A. L. Rheingold, L. C. Francesconi, *Inorg. Chem.* **2001**, *40*, 1894–1901.
[6] T. Kurata, A. Uehara, Y. Hayashi, K. Isobe, *Inorg. Chem.* **2005**, *44*, 2524–2530.
[7] Y. Hayashi, T. Shinguchi, T. Kurata, K. Isobe in *Vanadium: The Versatile Metal* (Eds.: K. Kustin, J. C. Pessoa, D. C. Crans), Oxford University Press, **2007**, ch. 29, pp. 408–423.
[8] a) H. Nakano, T. Ozeki, A. Yagasaki, *Inorg. Chem.* **2001**, *40*, 1816–1819; b) H. Nakano, T. Ozeki, A. Yagasaki, *Acta Crystallogr., Sect. C* **2002**, *58*, m464–m465; c) P. Román, A. S. José, A. Luque, J. M. Gutiérrez-Zorrilla, *Inorg. Chem.* **1993**, *32*, 775–776.
[9] a) A. Bino, S. Cohen, C. Heitner-Wirguin, *Inorg. Chem.* **1982**, *21*, 429–431; b) S. M. Baxter, P. T. Wolczanski, *Inorg. Chem.* **1989**, *28*, 3263–3264; c) C. Heitner-Wirguin, J. Selbin, *Inorg. Nucl. Chem.* **1968**, *30*, 3181–3188.
[10] T. Kurata, Y. Hayashi, K. Isobe, *Chem. Lett.* **2009**, 218–219.
[11] I. D. Brown in *The Chemical Bond in Inorganic Chemistry*, Oxford University Press, New York, **2002**.
[12] a) M. Volpe, H. Hartnett, J. W. Leeland, K. Wills, M. Ogunshun, B. J. Duncombe, C. Wilson, A. J. Blake, J. McMaster, J. B. Love, *Inorg. Chem.* **2009**, *48*, 5195–5207; b) M. Risch, V. Khare, I. Zaharieva, L. Gerencser, P. Chernev, H. Dau, *J. Am. Chem. Soc.* **2009**, *131*, 6936–6937.
[13] D. H. Busch, N. W. Alcock, *Chem. Rev.* **1994**, *94*, 585–623.
[14] K. Domae, D. Uchimura, Y. Koyama, S. Inami, Y. Hayashi, K. Isobe, H. Kameda, T. Shimoda, *Pure Appl. Chem.* **2009**, *81*, 1323–1330.
[15] T. Shimoda, Y. Matsuki, M. Furusawa, T. Aoki, I. Yudasaka, H. Tanaka, H. Iwasawa, D. Wang, M. Miyasaka, Y. Takeuchi, *Nature* **2006**, *440*, 783–786.
[16] D. Coucouvanis, *Inorganic Syntheses*, Wiley, New York, **2002**, vol. 33, pp. 75–83.
[17] S. I. Zabinsky, J. J. Rehr, J. J. Ankudinov, R. C. Albers, M. J. Eller, *Phys. Rev. B* **1995**, *52*, 2995–3009.
[18] *CrystalClear*, version 1.3.5, Rigaku Corporation, Tokyo, Japan.
[19] G. M. Sheldrick, *SHELXL-97: Program for the Refinement of Crystal Structures*, University of Göttingen, Göttingen, Germany, **1997**.

Received: June 30, 2009
Published Online: November 2, 2009

